

Transistors with chemically synthesized layered semiconductor WS₂ exhibiting 10⁵ room temperature modulation and ambipolar behavior

Wan Sik Hwang,^{1,a)} Maja Remskar,² Rusen Yan,¹ Vladimir Protasenko,¹ Kristof Tahy,¹ Soo Doo Chae,¹ Pei Zhao,¹ Aniruddha Konar,¹ Huili (Grace) Xing,¹ Alan Seabaugh,¹ and Debdeep Jena^{1,b)}

¹Department of Electrical Engineering, University of Notre Dame, Notre Dame, Indiana 46556, USA

²Solid State Physics Department, Jozef Stefan Institute, Jamova 39, SI-1000 Ljubljana, Slovenia

(Received 30 March 2012; accepted 18 June 2012; published online 3 July 2012)

We report the realization of field-effect transistors (FETs) made with chemically synthesized multilayer crystal semiconductor WS₂. The Schottky-barrier FETs demonstrate ambipolar behavior and a high ($\sim 10^5 \times$) on/off current ratio at room temperature with current saturation. The behavior is attributed to the presence of an energy bandgap in the ultrathin layered semiconductor crystal material. The FETs also show clear photo response to visible light. The promising electronic and optical characteristics of the devices combined with the chemical synthesis, and flexibility of layered semiconductor crystals such as WS₂ make them attractive for future electronic and optical devices. © 2012 American Institute of Physics. [<http://dx.doi.org/10.1063/1.4732522>]

The continued success of modern electronic devices has been driven by scaling down of the active area such as the channel length and the gate dielectric thickness. As device sizes continue to shrink, short channel effects lead to poor threshold control.¹ The origin of such effects is linked to the 3-dimensional (3D) nature of semiconductors used to make the transistors. Silicon-on-insulator (SOI) technology was introduced in order to reduce device degradation due to short-channel effects by rendering the active semiconducting material more two-dimensional.² The recently discovered material graphene³ on the other hand is a true two-dimensional (2D) material with a single atomic sheet of graphite that is highly attractive for scaling from electrostatics viewpoint, but has a zero energy band gap. It has sparked intense research for electronic device applications due to its exceptionally high mobility (excess of 15 000 cm²/Vs) at room temperature and high Fermi velocity,⁴ yet the absence of an energy gap prevents it from traditional electronic switching since it cannot be switched off. Efforts to overcome this problem involve the opening of bandgaps by quantum confinement in graphene nanoribbons (GNRs).⁵ The size of the energy gap is inversely proportional to the width of the GNR.⁶ GNR field-effect transistors (FETs) using exfoliated graphene,^{6,7} epitaxial graphene,⁸ or chemical vapor deposition (CVD) grown graphene⁹ close to ~ 10 nm widths still exhibit low I_{ON}/I_{OFF} ratios at room temperature due to the small gaps; the effect of edge disorder and the absence of current saturation currently are proving major challenges. Novel device concepts such as interlayer tunneling FETs may help graphene based FETs achieve better switching in the near future,^{10,11} but the zero-gap nature of 2D graphene remains a hindrance for traditional planar FET realization with this 2D crystal.

Spurred by the knowledge of isolation of graphene, other 2D transition-metal dichalcogenide materials in the

form of MX₂ (where M = transition metal such as Mo, W, Ti, Nb, etc. and X = S, Se, or Te) have drawn considerable attention. The multilayer forms of these materials, like graphite, are traditionally used as lubricants or intercalated batteries due to their layered structure and are thus chemically synthesized in large volumes. The MX₂ material family consists of one or more sets of triple layers with one M and two X atoms in a sandwich structure (X-M-X layers). Atoms within each layer are strongly held together by covalent-ionic mixed bonds, while interlayer van der Waals forces are weak. Substantial prior works in multilayered materials have concentrated on their optical and material properties.^{12–14} FETs using MoS₂ and WSe₂ have been demonstrated with substantial gate modulation.^{15,16} A recent calculation showed that single layer WS₂ has the potential to outperform Si and other 2D crystals in FET-type applications due to its favorable bandstructure.¹⁷ No prior device results have been yet reported for WS₂ for either logic or optical applications. In this letter, we report the first fabrication and demonstration of ultrathin WS₂ FETs on chemically synthesized material. We also preliminary results on the effects of photo-excitation on the transistor characteristics.

WS₂ flakes were grown by an iodine-transport method from previously synthesized WS₂ (0.6 g) at 1060 K in evacuated silica ampoule at pressure of 10⁻³ Pa, and with temperature gradient of 6.8 K/cm. The volume concentration of iodine was 11 mg/cm³. After 21 days of growth, the silica ampoule was slowly cooled to room temperature with a controlled cooling rate of 30 °C/h. The WS₂ flakes were then dispersed by sonication in isopropyl alcohol (IPA) and deposited on 30 nm atomic-layer-deposited (ALD) Al₂O₃/p-Si substrates at 100 °C for drying. A schematic cross-sectional image of the back-gated WS₂ device is shown in Fig. 1(a). The source and drain contacts are defined by electron beam lithography (EBL) using Ti/Au (5/100 nm) contacts. An atomic force microscope (AFM) image of the WS₂ device with $L/W = 2.5/2 \mu\text{m}$ is shown in Fig. 1(b), and the width of the channel region is $\sim 2 \mu\text{m}$. The cross-sectional height of

^{a)}whwang1@nd.edu.

^{b)}djena@nd.edu.

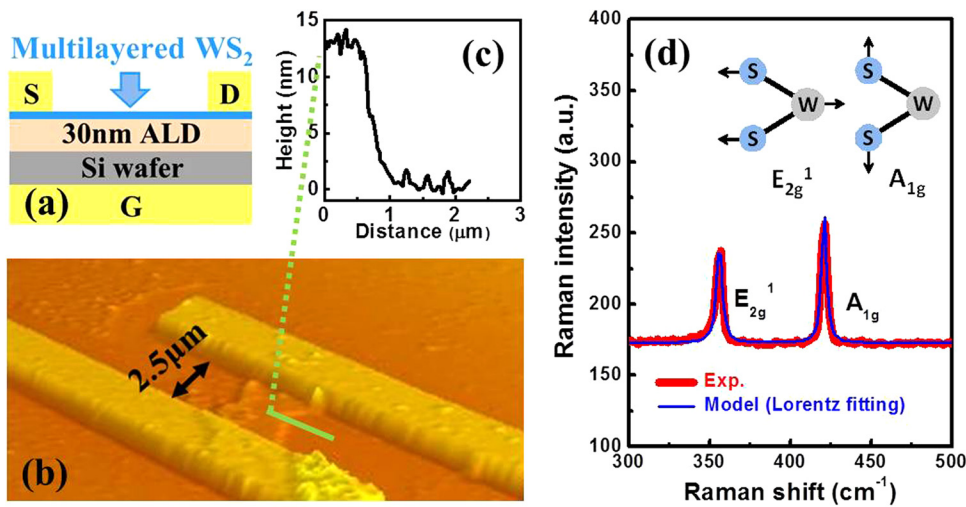


FIG. 1. (a) Schematic cross-sectional image of a WS₂ transistor with multilayered WS₂. (b) AFM image of the device on top of 30 nm Al₂O₃ layer with Ti/Au contacts. (c) Cross-sectional height of WS₂ layer indicated by green line of (b) by AFM. (d) Raman spectra ($\lambda = 488$ nm) of the multilayered WS₂ with laser power of 1.5 mW. The inset sketch shows the two primary vibrational modes of WS₂ leading to the two peaks in the Raman spectrum.

the WS₂ layers is ~ 13 nm which is equivalent to 18–20 single layers, since the interlayer spacing of WS₂ is in the range of 0.65–0.70 nm.¹⁸ The Raman spectra ($\lambda_{\text{exc}} = 488$ nm) of the WS₂ region as shown in Fig. 2(d) exhibit two peaks: one in the E_{2g}¹ range for in-plane vibrations at ~ 356 cm⁻¹ and the other in the A_{1g} range for out-of-plane vibrations at ~ 421 cm⁻¹.¹⁹ The laser spot is aligned to the channel region with spot size of 0.5–1 μm and laser power of ~ 1.5 mW. The Raman signal is fit to two single Lorentzian models, revealing that the chemical-transport-growth ultrathin WS₂ materials effectively retain the single-crystal properties of WS₂ with unnoticeable structural modifications.

Figure 2(a) shows the measured drain current I_D versus the gate-source voltage V_{GS} at room temperature for a multilayer WS₂ device at two drain biases. The gate modulation is $\sim 10^5 \times$ for $V_{DS} = 1$ V, and $\sim 10^4$ for $V_{DS} = 5$ V. The gate leakage current is much lower (\sim few pA) than the drain current and is not shown for clarity. The device shows clear ambipolar behavior indicating accumulation of electrons (n-type conductivity) for positive V_{GS} and of holes (p-type conductivity) for negative V_{GS} regions. Thus, electron and hole carriers are preferentially injected depending on the

gate bias as illustrated in the inset of Fig. 2(a) as a consequence of Schottky barrier contacts. This is seen clearly in the family of $I_D - V_{DS}$ curves in Fig. 2(b). The high resistance of the Schottky barrier contacts also makes it difficult to extract important parameters like carrier mobilities in a transparent manner from the field-effect behavior. It is expected that low-resistance ohmic contacts will be possible for WS₂ in the near future. Several methods are available to suppress one of the carriers to make the devices less ambipolar to decrease the I_{off} and improve the modulation.^{20,21} Nevertheless, the ambipolar behavior can be advantageous for CMOS-like inverter applications²² or for analog frequency multiplication purposes.²³ The energy band line-ups as shown in the inset of Fig. 2(b) indicate that Fermi level of the contact metal is aligned in the band gap of WS₂. The contact metal consists of Ti/Au (5/100 nm), and though the work function of Ti is 4.3 eV, if the thickness of metal (Ti in this work) is less than 5 nm, the net work function of the metal stack can be influenced by the 2nd metal (Au in this work).^{24,25} The family of $I_D - V_{DS}$ curves at various V_{GS} in Fig. 2(b) shows current saturation, a feature enabled by the substantial bandgap. The saturation of current is attributed to

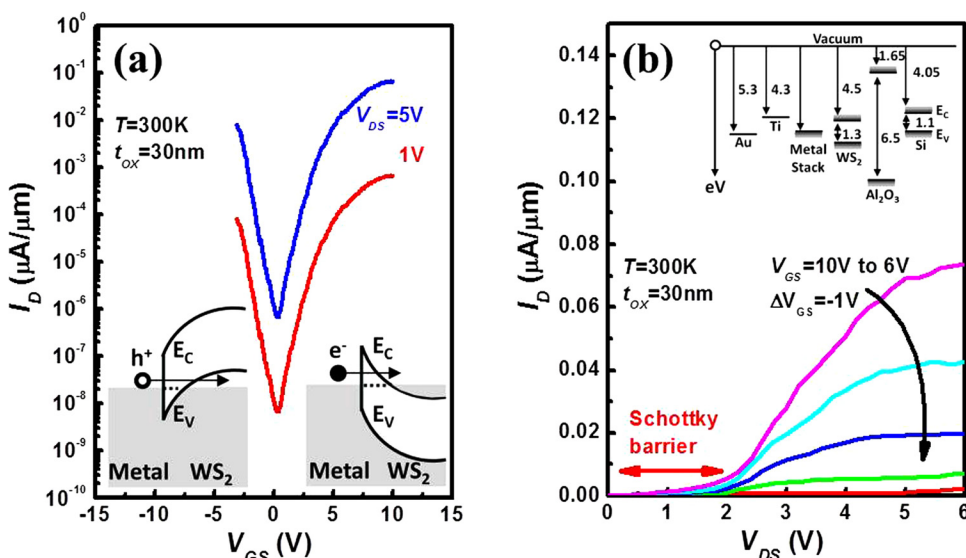


FIG. 2. (a) Drain current I_D vs. back gate voltage V_{GS} with $W/L = 2.0/2.5$ μm at various drain voltages V_{DS} , showing $\sim 10^5 \times$ on/off current ratio and ambipolar behavior. The inset sketch image shows a conduction mechanism of electrons or holes depending on the gate bias. (b) Drain current I_D vs. drain voltage V_{DS} indicating the presence of Schottky barrier limited-current and current saturation. The band diagram of inset image indicates the formation of Schottky barrier contact between metal and WS₂.^{26–28} The expected bandgap of multilayer WS₂ is ~ 1.3 eV, while the reported bandgap of a single layer is ~ 1.8 eV.²⁹ Typically, multilayer structures of layered semiconductors develop indirect bandgaps lower than their monolayer constituents.³⁰

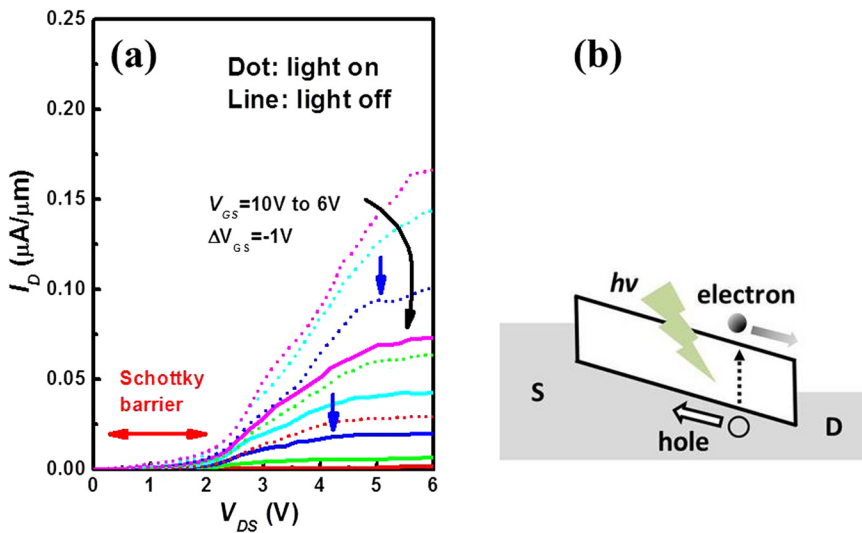


FIG. 3. (a) Dependence of drain current I_D vs. drain voltage V_{DS} at various gate voltages V_{GS} on illumination showing the photocurrent in WS₂ FETs. (b) A schematic representation of electron-hole pair generation upon photon absorption, and the increase of drain current due to conduction by these excess carriers.

pinch-off in the channel at the drain side, similar to long-channel transistors. Both the high on/off current ratio ($\sim 10^5 \times$) and current saturation over a wide voltage window are possible due to the presence of a bandgap, unlike graphene.

The optical properties of 1-dimensional WS₂ nanotubes have been investigated earlier and response to visible light has been reported.³¹ In the WS₂ flakes studied here, the photoresponse of the WS₂ Schottky barrier FETs was measured by illuminating the device with a halogen lamp; the result is shown in Fig. 3(a). Figure 3(b) shows a schematic representation of electron-hole pair generation upon photon absorption, and the increase of drain current due to conduction by these excess carriers. We observe that the saturation drain voltage increases under illumination, which can be attributed to the photogeneration of carriers. The increase in carrier density requires a higher drain voltage to achieve pinch-off in the channel near the drain side. A more careful photocurrent spectrum measurement can reveal the energy bandgap and its nature (direct or indirect) of multilayer WS₂, which is suggested as a future work. We also ensure that the photocurrent is caused by WS₂ and not the Si substrate, since once the illumination beam is focused outside the WS₂ channel region, the photocurrent effect disappears. The gate leakage of the device is lower than drain current by more than 3 orders of magnitude in this experiment.

In summary, ultrathin WS₂ transistors were fabricated and characterized for the first time from chemically synthesized material. Raman measurements prove the crystal nature of the layered semiconductor material. The presence of a bandgap leads to high on/off current ratios and current saturation in the transistors at room temperature. In addition, the observed photoresponse of the multilayered semiconductor can enable optical device applications. This initial report on the behavior of chemically synthesized WS₂ expands the family of layered semiconductors that possess the features for enabling a wide range of electronic and optical applications. A large amount of work is necessary to form low resistance ohmic contacts and to control the thickness and uniformity of the WS₂; the initial observations presented here provide sufficient motivation to move in that direction.

This work was supported by the Semiconductor Research Corporation (SRC), Nanoelectronics Research Initiative (NRI), and the National Institute of Standards and Technology (NIST) through the Midwest Institute for Nanoelectronics Discovery (MIND), the Office of Naval Research (ONR), and the National Science Foundation (NSF). We thank J. Jelenc for technical help in crystal growth, Slovenian Research Agency of the Republic of Slovenia, for financial support, Contract No. J1-2352, and the Centre of Excellence NAMASTE.

¹K. Bjorkqvist and T. Amborg, *Phys. Scr.* **24**, 418 (1981).

²S. Veeraghavan and J. G. Fossum, *IEEE Trans. Electron Devices* **36**, 522 (1989).

³K. S. Novoselov, A. K. Geim, S. V. Morozov, D. Jiang, Y. Zhang, S. V. Dubonos, I. V. Grigorieva, and A. A. Firsov, *Science* **306**, 666 (2004).

⁴A. K. Geim and K. S. Novoselov, *Nature Mater.* **6**, 183 (2007).

⁵K. Nakada, M. Fujita, G. Dresselhaus, and M. S. Dresselhaus, *Phys. Rev. B* **54**, 17954 (1996).

⁶M. Y. Han, B. Ozyilmaz, Y. Zhang, and P. Kim, *Phys. Rev. Lett.* **98**, 206805 (2007).

⁷K. Tahy, T. Fang, P. Zhao, A. Konar, C. Lian, H. G. Xing, M. Kelly, and D. Jean, "Graphene transistors," in *Physics and Applications of Graphene—Experiments*, edited by Sergey Mikhailov (InTech, 2011), chap. 20, p. 475.

⁸W. S. Hwang, K. Tahy, L. O. Nyakiti, V. D. Wheeler, R. L. Myers-Ward, C. R. Eddy, Jr., D. K. Gaskill, H. G. Xing, A. Seabaugh, and D. Jena, *J. Vac. Sci. Technol. B* **30**, 03D104 (2012).

⁹W. S. Hwang, K. Tahy, X. Li, H. G. Xing, A. Seabaugh, C.-Y. Sung, and D. Jena, *Appl. Phys. Lett.* **100**, 203107 (2012).

¹⁰R. M. Feenstra, D. Jena, and G. Gu, *J. Appl. Phys.* **111**, 043711 (2012).

¹¹L. Britnell, R. V. Gorbachev, R. Jalil, B. D. Belle, F. Schedin, A. Mishchenko, T. Georgiou, M. I. Katsnelson, L. Eaves, S. V. Morozov, N. M. R. Peres, J. Leist, A. K. Geim, K. S. Novoselov, and L. A. Ponomarenko, *Science* **335**, 947 (2012).

¹²G. L. Frey, S. Elani, M. Homyonfer, Y. Feldman, and R. Tenne, *Phys. Rev. B* **57**, 6666 (1998).

¹³E. Gourmelon, O. Lignier, H. Hadouda, G. Couturier, J. C. Bernede, J. Tedd, J. Pouzet, and J. Salardenne, *Sol. Energy Mater. Sol. Cells* **46**, 115 (1997).

¹⁴M. Krause, M. Virsek, M. Remskar, A. Kokitsch, and W. Moller, *Phys. Status Solidi B* **246**, 2786 (2009).

¹⁵B. Radisavljevic, A. Radenovic, J. Brivio, V. Giacometti, and A. Kis, *Nat. Nanotechnol.* **6**, 147 (2011).

¹⁶V. Podzorov, M. E. Gershenson, Ch. Kloc, R. Zeis, and E. Bucher, *Appl. Phys. Lett.* **84**, 3301 (2004).

¹⁷L. Leitao, S. B. Kumar, O. Yijian, and G. Jing, *IEEE Trans. Electron Devices* **58**, 3042 (2011).

- ¹⁸H. S. S. Ramakrishna Matte, A. Gomathi, A. K. Manna, D. J. Late, R. Datta, S. K. Pati, and C. N. R. Rao, *Angew. Chem., Int. Ed.* **49**, 4059 (2010).
- ¹⁹C. Sourisseau, F. Cruege, M. Fouassier, and M. Alba, *Chem. Phys.* **150**, 281 (1991).
- ²⁰V. Derycke, R. Martel, J. Appenzeller, and Ph. Avouris, *Nano Lett.* **1**, 453 (2001).
- ²¹Y.-M. Lin, J. Appenzeller, and Ph. Avouris, *Nano Lett.* **4**, 947 (2004).
- ²²W. J. Yu, U. J. Kim, B. R. Kang, I. H. Lee, E.-H. Lee, and Y. H. Lee, *Nano Lett.* **9**, 1401 (2009).
- ²³W. Han, A. Hsu, J. Wu, K. Jing, and T. Palacios, *Electron Device Lett.* **31**, 906 (2010).
- ²⁴W. S. Hwang, D. S. H. Chan, and B. J. Cho, *IEEE Trans. Electron Devices* **55**, 2469 (2008).
- ²⁵H. P. Yu, K. L. Pey, W. K. Choi, D. A. Antoniadis, E. A. Fitzgerald, D. Z. Chi, and C. H. Tung, *Appl. Phys. Lett.* **89**, 233520 (2006).
- ²⁶*New Trends in Intercalation Compounds for Energy Storage*, edited by C. Julien, J. P. Pereira-Ramos, and A. Momchilov (Kluwer Academic, Dordrecht, 2002), p. 215.
- ²⁷W. Jaegermann, in *Photoelectrochemistry and Photovoltaics of Layered Semiconductors*, edited by A. Aruchamy (Kluwer Academic, Dordrecht, 1992), pp. 195–282.
- ²⁸*CRC Handbook on Chemistry and Physics* edited by William M. Haynes (CRC Press, 2008), pp. 12–114.
- ²⁹A. Kuc, N. Zibouche, and T. Heine, *Phys. Rev. B* **83**, 245213 (2011).
- ³⁰A. Splendiani, L. Sun, Y. Zhang, T. Li, J. Kim, C.-Y. Chim, G. Galli, and F. Wang, *Nano Lett.* **10**, 1271 (2010).
- ³¹H. E. Unalan, Y. Yang, Y. Zhang, P. Hiralal, D. Kuo, S. Dalal, T. Butler, S. N. Cha, J. E. Jang, K. Chremmou, G. Lentaris, D. Wei, R. Rosentsveig, K. Suzuki, H. Matsumoto, M. Minagawa, Y. Hayashi, M. Chhowalla, A. Tanioka, W. I. Milne, R. Tenne, and G. A. J. Amaratunga, *IEEE Trans. Electron Devices* **55**, 2988 (2008).